Parallel Reconstruction of Quad Only Meshes from Volume Data

Roberto Grosso and Daniel Zint
Visual Computing, Friedrich-Alexander-Universität Erlangen-Nürnberg (FAU), Germany

Keywords: Dual Marching Cubes, Quad Meshing, Parallel Mesh Reconstruction.

Abstract: We present a method to reconstruct quad only meshes from volume data which mainly consists of two steps: reconstruction of a quad only mesh and topological simplification to reduce the number of irregular vertices. A novel algorithm is described that computes Dual Marching Cubes (DMC) meshes without using lookup tables. The meshes are topologically consistent across cell borders, i.e. they are watertight. The output of the algorithm is a quad only mesh stored in a halfedge data structure. Due to the transitions between voxel layers in volume data, meshes have numerous quad elements with vertices of valence $3-X-3-Y$, where $X,Y \geq 5$, and $3-3-3-3$. Hence, we simplify the mesh by eliminating these elements wherever possible. Finally, we briefly describe a CUDA implementation of the algorithms, which allows processing huge amounts of data on GPU at almost interactive time rates.

1 INTRODUCTION

Iso-surface reconstruction from volume data is a common processing step in many engineering and scientific applications, such as surface reconstruction from range sensor data, analysis and visualization of medical images, or geometry reconstruction of large protein chains in molecular science. In many cases, volume data is represented by a hexahedral mesh which stores a scalar function sampled at the mesh vertices. In medical applications CT or MRI data are represented by voxel grids. In this work cell means a voxel or a hexahedral mesh element. The surface is obtained by the Marching Cubes (MC) algorithm, which only requires an iso-value representing the surface as input. A MC surface shows two major drawbacks. Triangles are poorly shaped, and the mesh is not topologically correct, i.e. it might be inconsistent across cell borders and not homeomorphic to the underlying surface (Nielson, 2003). The dual marching cubes (DMC) algorithm (Nielson, 2004) generates quad only meshes. It is based on a lookup table with 23 base cases. A consistent discretization of the iso-surface across cell borders requires using the asymptotic decider (Nielson and Hamann, 1991; Grosso, 2017) which results in a large number of special cases, called subconfigurations in (Nielson, 2003). An alternative strategy to generate consistent triangulations of the iso-surface was presented in (Grosso, 2016a; Renbo et al., 2005; Pasko et al., 1988) and is based on the following observations. Given an iso-value ι_0, the iso-surface is defined as:

$$S_{\iota_0} = \{(x,y,z) \in \mathbb{R}^3 | T(x,y,z) = \iota_0\}, \qquad (1)$$

where $T : \mathcal{M} \to \mathbb{R}$ is the trilinear interpolant defined on the hexahedral mesh $\mathcal{M}$. The intersection of the iso-surface with a face of a cell is a set of hyperbolic arcs. The intersection of the iso-surface with a cell is a set of closed curves, each being a C^0-continuous collection of hyperbolic arcs. Up to four different components or branches of the iso-surface can intersect a cell, resulting in up to four independent closed curves, hereafter referred to as *MC polygons*. They are consistent across cell borders if the asymptotic decider is applied.

DMC computes a *vertex representative* for each MC polygon, which should lie on the iso-surface defined by equation (1). In a hexahedral mesh an edge is shared by four cells. If we connect the vertex representatives of the cells sharing a common edge we obtain a quadrilateral. Thus, DMC generates quad only meshes. If the intersection of the iso-surface with a cell is computed using the asymptotic decider, it is guaranteed that the DMC mesh is topologically consistent across cell borders, i.e. it is watertight.

The main contribution of the work is a new DMC algorithm which does not require a lookup table, generates watertight meshes, and is simple to parallelize.

Grosso, R. and Zint, D.
Parallel Reconstruction of Quad Only Meshes from Volume Data.
DOI: 10.5220/0008948701020112
In *Proceedings of the 15th International Joint Conference on Computer Vision, Imaging and Computer Graphics Theory and Applications (VISIGRAPP 2020) - Volume 1: GRAPP*, pages 102-112
ISBN: 978-989-758-402-2; ISSN: 2184-4321

The algorithm output is a high quality quad only mesh which accurately represents the underlying geometry as defined by equation (1). Neighborhood and connectivity information is encoded using a halfedge data structure. Furthermore, we implemented parallel smoothing methods to reduce vertices and elements with valence pattern $3-X-3-Y$, $X,Y \geq 5$ and $3-3-3-3$ which commonly appear in DMC meshes computed from volume data.

In the following, we first present a brief review of previous work emphasizing the problem of topological consistency and parallel reconstruction. In Sec. 3 we present the parallel DMC algorithm, and in Sec. 4 we describe our parallel implementation of two mesh simplification techniques. In Sec. 5 we show the performance of the methods presented, and in Sec. 6 we give some comments on the results. The source code is available at GitHub (Grosso, 2016b).

2 RELATED WORK

Research contributions in the area of iso-surface extraction from volume data can be classified into three main groups, *standard* Marching Cubes (MC) and its extensions to resolve topological correctness and consistency; Dual Marching Cubes which extract quad meshes dual to the MC polygons; and Dual Contouring, which computes an iso-surface from the dual grid or the dual of an octree.

Methods for computing iso-surfaces based on the standard MC have to deal with the problem of inconsistent meshes across cell borders. Furthermore, MC methods might generate meshes which are not homeomorphic to the iso-surface as defined by equation (1). Methods presented so far are either based on extended lookup tables, or they first compute the intersection of the iso-surface with a cell, resulting in a MC polygon which is consistently triangulated.

After Dürst (Dürst, 1988) observed that MC does not consistently triangulate the iso-surface across cell borders, Nielson and Hamann (Nielson and Hamann, 1991) introduced the asymptotic decider to resolve ambiguities at the cell faces. Natarajan (Natarajan, 1994) discovered interior ambiguities and introduced an extended lookup table. Chernyaev (Chernyaev, 1995) modified the lookup table increasing the number of cases up to 33 in total, which is commonly called MC33. Different authors proposed new techniques to improve performance or to solve topological inconsistencies (Lewiner et al., 2003; Cignoni et al., 2000; Matveyev, 1999; Montani et al., 1994; Nielson, 2003; Custodio et al., 2013; Etiene et al., 2012; Lopes and Brodlie, 2003). For each ambiguous face, special subcases have to be considered which results in a large number of configurations.

Algorithms were presented which resolve ambiguities without using a lookup table. The first method to compute iso-surfaces based on the intersection of the surface with the cell faces was proposed by Pasko et al. (Pasko et al., 1988). Renbo et al. (Renbo et al., 2005) developed a triangulation algorithm which does not use lookup tables. These methods process unambiguous and ambiguous cells in the same manner, which is much more computational intensive than the MC algorithm. Grosso (Grosso, 2016a) developed a hybrid technique which processes unambiguous cells with the standard MC. Ambiguous cells are triangulated based on a set of rules applied to the MC polygons. This method has the advantage of not relying on lookup tables in ambiguous cases.

In order to improve performance and to overcome the problem of generating a large amount of triangles many parallel strategies were proposed in literature. A parallel iso-surface algorithm which is combined with edge collapses was presented in (Ulrich et al., 2014; Dupuy et al., 2010). It is a modification of the *tandem* algorithm introduced in (Attali et al., 2005). Parallel implementations become more complex if the output has to be a data structure with connectivity and neighborhood information. A GPU-based technique to reconstruct and smooth the iso-surface by repositioning the vertices without changing mesh topology was introduced in (Chen et al., 2015). A method to compute standard MC on multiple GPUs was described in (D'Agostino and Seinstra, 2015). A major problem of these algorithms is that they use large buffers to compute a consistent numbering of the vertex indices. Usually, a unique vertex index is computed by counting cells or edges via a prefix sum. This is not viable in our case, as buffers may become very large. We opted for a different technique which results in a much simpler algorithm that delivers good performance results and allows to compute iso-surfaces from very large volume data.

The Dual Marching Cubes algorithm presented by Nielson (Nielson, 2004) is a different strategy to reconstruct an iso-surface from a volume data. The intersection of the iso-surface with the cell can be approximated by a polygon on the cell faces. This is what we call the MC polygon in the previous section. The DMC algorithm computes the dual of these MC polygons. The dual to the MC polygons is a quad only mesh because each edge in the volume mesh is shared by four cells. This algorithm relies on the lookup table introduced in (Nielson, 2003) which consists of 23 basis cases. Ambiguities are resolved by introducing sub-configurations. This method is a generaliza-

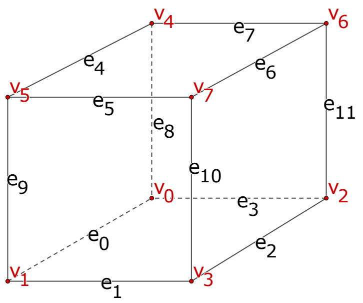

Figure 1: Local index convention for vertices and edges in a cell.

tion of the SurfaceNets proposed in (de Bruin et al., 2000; Gibson, 1998). A parallel implementation of the DMC algorithm is presented in (Löffler and Schumann, 2012). The method generates a 1-ring neighborhood data structure and approximates the surface by using error quadrics. Nevertheless, it relies on large buffers whose size depends on the number of edges to compute unique vertex indices via prefix sums.

Dual Contouring (DC) (Schaefer and Warren, 2004; Ju et al., 2002) is an alternative method for extracting iso-surfaces from volume data. It first approximates the data by computing an octree. For each cell of the octree, the method computes a single vertex representing the surface intersection with the cell. The vertex is placed within the cell by optimizing a quadratic functional based on error quadrics. The method just computes a single vertex for each cell in the octree, and therefore the resulting mesh might not be manifold. Subsequently different works were proposed that mainly deal with the problem of computing manifold meshes out of an octree (Rashid et al., 2016; Schaefer et al., 2007; Kazhdan et al., 2007; Zhang et al., 2004). Dual contouring generates triangle meshes from a hierarchical data structure.

3 DUAL MARCHING CUBES

We use the index convention for vertices and edges shown in Fig. 1. For instance, in the unit reference cell $[0,1]\times[0,1]\times[0,1]$ we have $v_0 = (0,0,0)$, and $e_0 = \{v_0, v_1\}$. The restriction of the trilinear interpolant T to a unit reference cell has the form

$$\begin{aligned} F(u,v,w) = \\ & (1-w)[f_0(1-u)(1-v)+f_1u(1-v) \\ & +f_2(1-u)v+f_3uv] \\ & +w[f_4(1-u)(1-v)+f_5u(1-v) \\ & +f_6(1-u)v+f_7uv]\,, \qquad (2) \end{aligned}$$

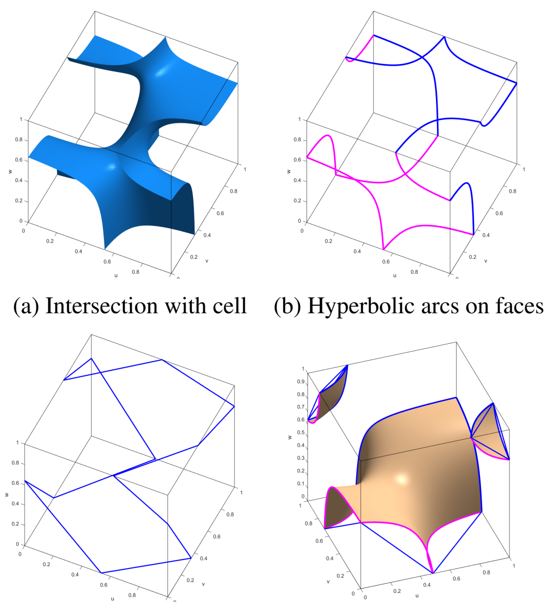

(a) Intersection with cell (b) Hyperbolic arcs on faces

(c) 12 sided MC polygon approximating the hyperbolic arcs (d) Three MC polygons

Figure 2: MC polygons approximating the intersection of the iso-surface with the cell faces.

where $(u,v,w)\in[0,1]^3$ are local coordinates and f_i are the function values at the cell vertices v_i. Up to four branches of the iso-surface obtained from $F(u,v,w)=\iota_0$ might intersect the cell. In Fig. 2a we show an iso-surface with only one component intersecting the cell at all twelve edges. In Fig. 2b we see the corresponding hyperbolic arcs at the cell faces, and in Fig. 2c the MC polygon used to approximate the hyperbolic arcs. For each branch of the iso-surface, DMC selects a single vertex within the cell which *represents* the surface. For the case shown in Fig. 2d three vertices have to be computed.

Each edge in the mesh or voxel grid is shared by four cells, except for the boundary edges. If a branch of the iso-surface intersects an edge, it will intersect all four cells sharing this edge. Therefore, connecting the representative vertices from each cell will generate a quadrilateral that is an element of the iso-surface. If the MC polygons are constructed using the asymptotic decider (Nielson and Hamann, 1991), the generated mesh is topologically consistent across cell borders. The mesh is called dual, because each vertex in the MC polygon has a corresponding quadrilateral in the dual mesh, and each vertex of the dual mesh represents a MC polygon. The DMC generates meshes which have less vertices and better shaped elements than the meshes generated by the standard MC algorithm (Nielson, 2004). Nevertheless, the generated

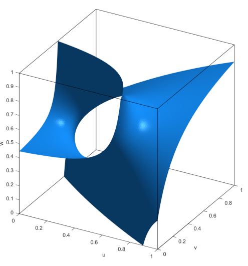
(a) MC case 12

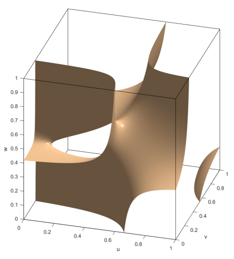
(b) MC case 13

Figure 3: Two configurations which have the topology of a cylinder (tunnel) for MC cases 12 and 13.

iso-surface might not be topologically correct. For certain configurations which can typically be found in medical data, the iso-surface (1) will not be homeomorphic to the reconstructed mesh. The DMC algorithm as it was formulated above cannot reconstruct tunnels (Grosso, 2016a), Fig. 3. The standard MC algorithm cannot reconstruct these tunnels either.

The parallel DMC algorithm we propose generates an indexed face set for the quadrilateral mesh, where the elements are all consistently oriented. Optionally, a halfedge data structure carrying neighbor information can be computed. The global structure of the algorithm we propose consists of three main steps: 1) initialize buffers; 2) compute the DMC mesh; 3) generate a halfedge data structure. In the initialization step buffers are created and default values are set with the help of simple CUDA kernels. In the next subsections we briefly describe how to compute the DMC quadrilateral mesh and subsequently generate the halfedge data structure.

3.1 DMC Quadrilateral Mesh

The DMC quadrilateral mesh is computed with two CUDA kernels. The first kernel proceeds cell wise and computes the vertex representatives and the quadrilaterals. The indices constituting a quadrilateral are stored by the kernel in a hash table. We opted to use a hash table to enable processing of volume data consisting of hundreds of millions of vertices, see Sec. 5. The second kernel collects the quadrilaterals from the hash table into an index buffer. Each thread started by the first kernel has to carry out the following processing steps for the cell being processed: 1) Compute MC polygons, 2) Estimate vertex representatives for each MC polygon, and 3) Compute and store quadrilateral indices in a hash table. In order to improve performance, the kernel returns immediately if the iso-surface does not intersect the cell.

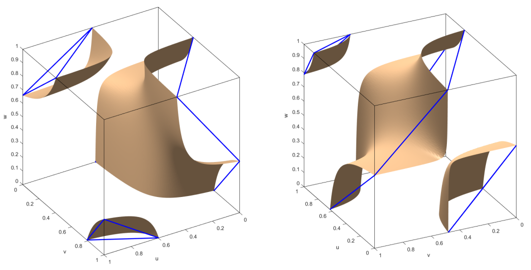
Figure 4: Two configuration where three branches intersect the cell, MC case 13.

3.1.1 Computation of MC Polygons

A cell might be intersected by up to four disconnected branches of the iso-surface. Therefore, we expect to obtain up to four closed MC polygons. The *device* method implemented for this purpose returns the number of polygons, the size of each of the polygons, and the indices of the intersected edges. This quantities can be computed in two steps. First, the cell is processed face wise. The intersection of the iso-surface with a face is given by a segment, Fig. 2. For each segment on a face the indices of the start and end edge are computed. Segments are oriented such that vertices with function values larger than the iso-value are located to the left of the segments. Ambiguous cases are solved with the asymptotic decider (Nielson and Hamann, 1991). In a second step, segments are connected to build up closed polygons. The number of MC polygons, their size, and the indices of the edges being intersected can be stored in a 64bit `unsigned long integer`.

3.1.2 Estimation of Vertex Representatives

Within the cell a vertex that is a representative of the iso-surface is computed for each surface branch. The vertex representative must be placed as close as possible to the iso-surface defined by equation (1). The different branches intersecting the cell might be very close to each other, Fig. 4. The estimates for the vertex representatives must be positioned on the right surface branch, otherwise the resulting mesh will be non-manifold, i.e. mesh elements will overlap. We compute these vertices in two steps. First, an initial position is estimated. Second, the vertex is moved towards the surface by iteration. The initial position of the vertex is computed as the mean value (center of gravity) of the vertices of the MC polygon. This is a good estimate as can be easily seen from the fact that branches of the surface within a cell are separated by asymptotic planes.

Next, the position of the representatives is moved towards the surface (1) by using the following iteration formula:

$$\mathbf{v}^{k+1} = \mathbf{v}^k + \lambda \nabla F(\mathbf{v}^k), \tag{3}$$

where $\mathbf{v} = (u, v, w)$ are the local coordinates and λ is given by

$$\lambda = \alpha \cdot \frac{\iota_0 - F(\mathbf{v}^k)}{||\nabla F(\mathbf{v}^k)||^2},$$

where α is a damping factor. We choose $\alpha = 0.25$ and iterate for a maximum of five steps. Normals are computed at the vertex representative in two steps. First, the gradient of the scalar function is estimated at the cell vertices by using central difference. Second, the gradient is interpolated trilinearly at the position of the vertex representative and then normalized. We use central differences because it has a better truncation error than forward or backward difference. The computation of the gradient using the trilinear interpolant has the same approximation error as forward difference, thus producing poor results.

3.1.3 Computation of the Quadrilaterals

Quadrilaterals are computed by connecting vertices of four neighbor cells sharing a common edge. The edge must be intersected by the corresponding MC polygons. Quadrilaterals must be consistently oriented. In contrast to the original MC lookup table (Lorensen and Cline, 1987), quadrilaterals are oriented such that their normals point in the same direction as the gradient of the volume data.

Each quadrilateral is uniquely assigned to an edge of the volume mesh. Quadrilaterals are stored in a hash table where the `key` is the unique index of the corresponding edge. We use open hashing and linear probing to find an empty bucket in the hash table. Hash tables were chosen to be twice as large as the expected number of elements in table. A quadrilateral is represented by an array of four integers. For each cell, the index of the vertex representative has to be stored at the right position within this array to construct quadrilaterals which are consistently oriented. We are using the naming convention presented in Fig. 1. Fig 5 demonstrates how to save vertex indices properly. Edge $e_0 = \{v_0, v_1\}$ is shared by four neighbor cells. In the other three cells it will have the names $e_4 = \{v_4, v_5\}$, $e_6 = \{v_3, v_7\}$, and $e_2 = \{v_2, v_3\}$. Assume that $f_0 \geq \iota_0$ and the index B of the vertex is stored at the first position of the index array. The thread processing the cell where this edge has the name e_4 has to store the index C of the vertex representative at the second position in the array. Similarly, the thread processing the cell where the edge has the name e_6 stores the index D at the third position and finally, the thread processing the cell where the edge has the name e_2 stores the vertex A at the fourth position. All possible cases are summarized in Table 1. Each quadrilateral is computed by four threads and stored in a hash table as `key, [B, A, D, C]`.

Table 1: How to build quadrilaterals depending on the edge configuration. The table indicates the position of the vertex index in the quadrilateral array.

edge $e = \{v_i, v_j\}$	case $f_i \geq \iota_0$	case $f_j \geq \iota_0$
$e_0 = v_0, v_1$	0	0
$e_1 = v_1, v_3$	0	0
$e_2 = v_2, v_3$	3	1
$e_3 = v_0, v_3$	3	1
$e_4 = v_4, v_5$	1	3
$e_5 = v_5, v_7$	1	3
$e_6 = v_6, v_7$	2	2
$e_7 = v_4, v_6$	2	2
$e_8 = v_0, v_4$	0	0
$e_9 = v_1, v_5$	3	1
$e_{10} = v_3, v_7$	2	2
$e_{11} = v_2, v_6$	2	2

A kernel is in charge of computing the vertex representatives from each cell. The kernel processes the input data cell wise. For each cell it computes the vertex representatives and corresponding normals for each branch of the iso-surface. These vertices are interior to the cell, thus the kernel can assign a unique global index to the vertices which is required by the mesh data structure. The index corresponds to the position of vertex and normal within a buffer and is obtained using `atomicAdd` on an *atomic* counter. As indicated above this unique address for vertex and normal is stored in a hash table, where the key is the unique index of the edge in the voxel grid being intersected by the corresponding surface branch. The bucket in the hash table has four entries containing the indices of the vertices which build a quadrilateral. The vertices are stored in order to build a consistently oriented quadrilateral according to the scheme given in Table 1. The hash table is implemented as an array. Collisions are solved by using open addressing with linear probing. We use `atomicCAS` to test for collisions. At the end the hash table contains all quadrilaterals in the mesh.

Finally, a second kernel will collect the quadrilaterals from the hash table and save the elements into an index buffer. Boundaries are easily handled by this kernel. A bucket in the hash table contains a quadrilateral or it is empty. If an entry in a bucket is an *invalid* index, the cell was a boundary cell. In this case no quadrilateral is generated.

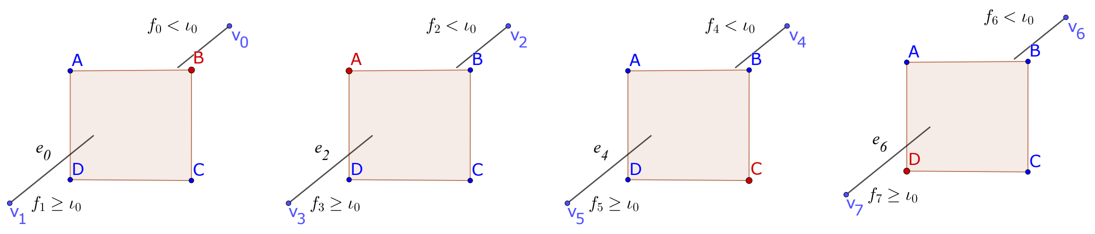

(a) case e_0 (b) case e_2 (c) case e_4 (d) case e_6

Figure 5: How to collect vertices from different cells which constitute a quadrilateral.

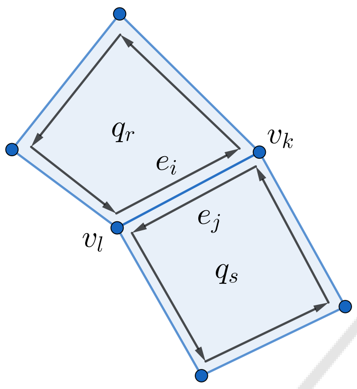

Figure 6: The distinct threads processing the twin edges e_i and e_j will compute the same `key` and save them in the same bucket in the hash table. The neighbor edges will be connected by the next kernel.

3.2 Halfedge Data Structure

The halfedge data structure is computed using two kernels. In the first kernel, each thread processes a quadrilateral and collects the *local* information required by the data structure. For each vertex we store the halfedge which starts at the vertex, and for the face the first halfedge is stored. For the four halfedges in a quadrilateral we store the index of the vertex at which the halfedge starts, the face and the index of the next halfedge. This kernel saves the indices of the halfedges in a hash table. The key is constructed using the indices of the incident vertices and saved in a 64bit `unsigned long int`. The smaller index is saved in the first 32bits, the larger index in the second 32bits. As shown in Fig. 6, distinct threads processing the *twin* edges e_i and e_j will compute the same `key` based on the indices of the vertices v_l, v_k and save them in the same bucket in the hash table. The haldedge whose starting vertex has the smaller index is store at the first entry in the bucket, the other at the second. Global information is collected by a second kernel which processes the entries of the hash table and connects *twin* edges. If a halfedge has no neighbor, it is a boundary edge.

4 MESH SIMPLIFICATION

Due to the transitions between layers in the volume data, the DMC mesh has numerous quadrilaterals with the valence pattern $3-X-3-Y$, where $X, Y \geq 5$, i.e. two non consecutive vertices with valence 3 and the other two vertices with valence equal to or larger than 5, Fig. 7a; and quadrilaterals with the valence pattern $3-3-3-3$, Fig. 7b. This elements can be easily removed from the mesh as follows. For the case 7a vertices in red are merged into a new vertex and the red element is removed. For the case 7b edges in red are collapsed moving vertices in red toward vertices in blue. The red elements are removed. For the configuration 7c no element can be removed in order to keep the mesh manifold.

4.1 Pattern $3-X-3-Y$

First note that if two neighbor elements with this valence pattern share a vertex of valence three, the elements can't be removed from the mesh. Otherwise, elements with this valence pattern are removed from the mesh with the following CUDA kernels:

1. Compute vertex valence. For this purpose a kernel iterates through the halfedges and increases the valence of its vertex by using `atomicAdd()`.
2. Find elements with the valence pattern. For each quadrilateral a kernel checks the element for the valence pattern. There is a buffer with an `int` entry for each vertex, a `counter`, which counts how often quadrilaterals with this valence pattern share a vertex with valence three. This way neighbor elements with the same valence pattern that can't be removed are identified easily.
3. Merge vertices with valence three. This kernel works element wise. For elements with this valence pattern the two vertices with valence three are merged into a new vertex, Fig. 7a, if the counter is one for both vertices. Otherwise, a neighbor element with this valence pattern shares

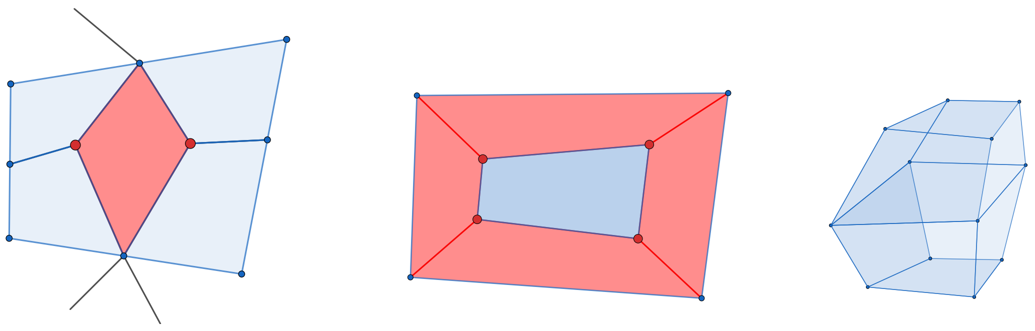

(a) Valence pattern $3-X-3-Y$, $X,Y \geq 5$ (b) Valence pattern $3-3-3-3$ (c) This configuration can't be removed

Figure 7: Valence pattern $3-X-3-Y$, where $X,Y \geq 5$ and $3-3-3-3$. For the case 7a on the left vertices in red are collapsed into a new vertex, removing the red element. For the case 7b in the middle the edges in red are collapsed moving the vertices in red toward the vertices in blue. The red elements are removed. For the configuration on the right no element will be removed in order to keep the mesh manifold.

a vertex of valence three, the element can't be removed.

4. Remove vertices. This kernel works vertex wise. It copies vertices to a new vertex buffer, if they are not marked for removal, and it maps old to new vertex indices.
5. Remove quadrilaterals. This kernel works element wise and copies quadrilaterals to a new element buffer, if they are not marked for removal. It uses index mapping from the previous kernel to connect vertices which form a quadrilateral.
6. Re-build halfedge data structure.

The algorithm requires five kernels to remove vertices and elements. Afterwards, the halfedge data structure has to be re-computed.

4.2 Pattern $3-3-3-3$

There are two configurations for which elements with this valence pattern can't be removed from the mesh: two neighbor elements have the same valence pattern, e.g. they are the faces of a hexahedron; or the elements are faces of a configuration as shown in Fig. 7c. In the latter case, two quadrilaterals sharing the same four vertices would remain, i.e. the mesh would be non-manifold. The following processing steps were implemented to remove elements with the valence pattern $3-3-3-3$:

1. Compute vertex valence. Similar to the kernel presented in Sec. 4.1.
2. Mark vertices and elements for removal. This kernel processes the mesh element wise. For each element it tests if all the vertices have valence three. In this case, the complete neighborhood is reconstructed. The kernel checks if the element has a neighbor with the same valence pattern or if it is the case shown in Fig. 7c. If not, the element and its four neighbors, Fig. 7b, are marked for removal.
3. Remove vertices. Similar to the kernel presented in Sec. 4.1.
4. Remove elements. Similar to the kernel presented in Sec. 4.1.
5. Re-compute halfedge data structure.

The algorithm requires four kernels to remove elements from the mesh. We remark that neighborhood is reconstructed using the halfedge data structure.

5 RESULTS

We evaluate the performance of the parallel DMC and simplification algorithms presented in this work. We compute the iso-surface from two CT data sets, a human skull of size $512^2 \times 641$ shown in Fig. 8 and a human torso of size $512^2 \times 743$ for which iso-surfaces were extracted with different iso-values. For the iso-value 700, Fig. 9a, we call the data *body*, and for the iso-value 1200 *skeleton*, Fig. 9b. The experiments were carried out on a desktop computer with an Intel Core i7-6700 with 32 GB memory and a NVIDIA GeForce GTX 1080 8GB. We first analyze the performance of the parallel DMC algorithm and afterwards present the effects of mesh simplification.

5.1 Parallel DMC

The performance of the parallel DMC is evaluated by measuring computation time and number of vertices and quadrilaterals generated. We compare the

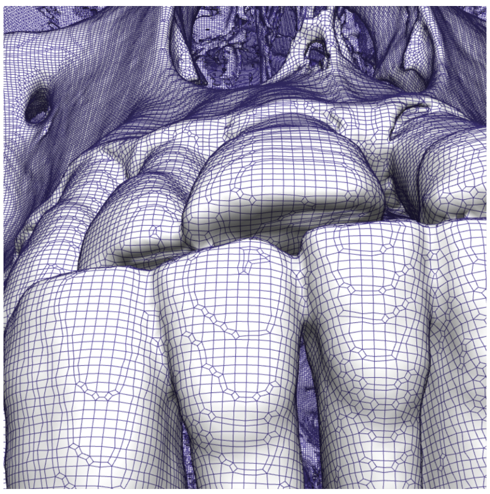
Figure 8: DMC mesh of a CT of a human skull after simplification.

results with the corresponding meshes obtained with the standard MC algorithm. For this purpose we subdivide quadrilaterals into triangles. For each element we select the subdivision which satisfies the MaxMin angle criterion. We also compare the quality of the elements generated by both algorithms. Element quality is computed using the mean ratio metric,

$$q_{\mathrm{m_{tri}}} = 4\sqrt{3}\frac{A}{\sum_{i=1}^{3} l_i^2}, \tag{4}$$

where A is the signed area of the triangle, and l_i is the length of their incident edges (Freitag and Knupp, 2002; M. Knupp, 2000).

Performance of the DMC in comparison with the standard MC is given in Table 2. Times are given in milliseconds. Both algorithms run on the GPU and for comparison both generate a shared vertex data structure. Table 3 gives the number of elements generated by DMC compared to the standard MC algorithm. DMC generates about 1% less vertices and correspondingly less elements than the standard MC. The standard MC algorithm is faster than the DMC algorithm. Nevertheless, it does not generate consistent meshes and the overall quality of the elements is worse compared to the elements generated by DMC as shown in Fig. 10. This figure shows the element quality for DMC with mesh simplification in cyan, without mesh simplification in magenta, and for MC in red. In this figure, elements are sorted according to their quality. We clearly see that the standard MC generates a much larger amount of triangles with a lower quality than the DMC. Mesh simplification slightly increases element quality. For comparison, quadrilaterals were subdivided into two triangles using the MaxMin angle criterion. Some quadrilaterals are thin resulting in triangles which don't have a good quality. Element quality and mesh consistency has a high impact in photo realistic high quality rendering in graphics applications or mesh processing in computational geometry. This is a main reason why dual methods for surface reconstruction are preferred over the standard MC algorithm. Performance was compared with a C++ implementation of DMC including a OpenMP parallelization using `omp` pragmas. The code has many critical areas due to unique index computations and writing operations. The GPU version is 60 to 77 times faster than the C++ OMP implementations and around 120 times faster than the sequential version as shown in Table 4. The back projection method introduced in Sec. 3.1, equation (3), improves the accuracy of the DMC mesh, Fig. 11. The plot in red corresponds to the approximation error without the projection of the vertex to the surface. The plot in blue is the error after projection. The approximation error is measured by comparing the function value at the vertex with the iso-value normalized to $[0,1]$. We clearly see that the point back projection improves the accuracy of the vertex representatives.

Table 2: Processing time to extract an iso-surface with the DMC and MC algorithms. The table includes the times required to generate the halfedge data structure from the DMC mesh.

	skull	body	skeleton
DMC	85	103	109
MC	54	68	74
halfedge	71	59	87

Table 3: Number of elements generated with the DMC and MC algorithms. The head data set has $512^2 \times 641$ voxels. The data set used to generate the the torso and body surfaces has $512^2 \times 743$ cells.

	vertices	elements
skull DMC	5,052,520	5,072,697
skull MC	5,072,707	10,239,432
body DMC	4,249,113	4,234,305
body MC	4,251,835	8,472,218
skeleton DMC	6,294,356	6,278,397
skeleton MC	6,291,993	12,555,936

Table 4: Processing time to extract an iso-surface with the DMC algorithm on GPU and CPU, including a CPU parallel implementation with OpenMP. Times are given in milliseconds.

	skull	body	skeleton
CUDA	85	103	109
CPU + OMP	6268	5415	8584
CPU	12204	13591	14523

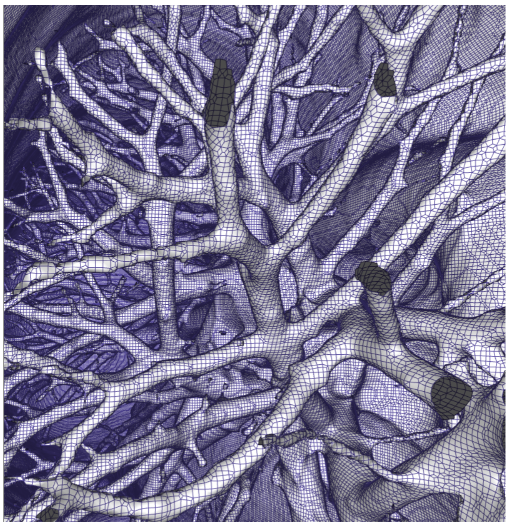
(a) DMC mesh showing respiratory tract, iso-value = 700

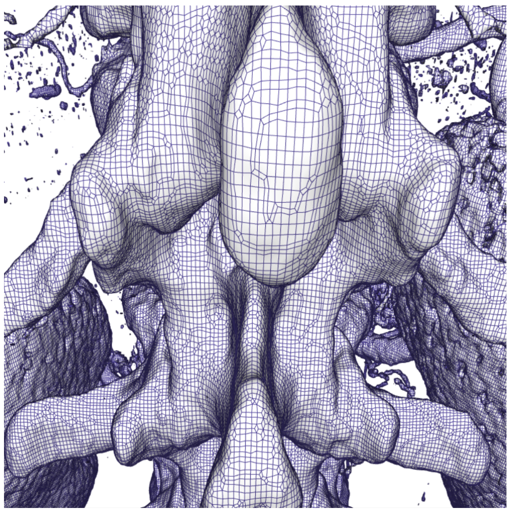
(b) DMC mesh showing the spine, iso-value = 1200

Figure 9: DMC mesh of a CT of a human torso.

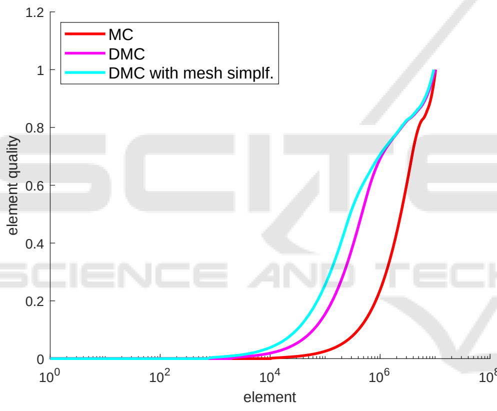

Figure 10: Element quality of DMC in cyan and magenta compared to MC in red based on the mean ratio metric.

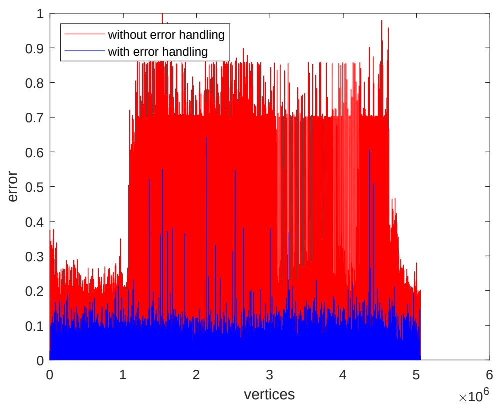

Figure 11: The red plot gives the error of the vertex representatives without back projection. The blue plot is the error after back projection.

5.2 Mesh Simplification

Simplification algorithms are evaluated by computational performance and by the number of elements being eliminated. The histograms presented in Fig. 12 show that the elimination of elements with valence patterns $3-X-3-Y$, $X,Y \geq 5$, and $3-3-3-3$ considerably reduces the number of irregular vertices.

Table 5: Simplification of elements with valence pattern $3-X-3-Y$. Times are given in milliseconds.

$3-X-3-Y$	skull	body	skeleton
time	12	9	14
vertices	169,331	161,904	212,795

Table 6: Simplification of the valence pattern $3-3-3-3$. Times are given in milliseconds.

$3-3-3-3$	skull	body	skeleton
time	7	5	8
vertices	190,292	18,652	165,908

The method implemented to simplify elements with the valence pattern $3-X-3-Y$, where $X,Y \geq 5$ eliminates the same number of vertices and elements. Table 5 gives runtime and total number of elements removed from the original DMC mesh. For instance, for the human skull data set it reduces about 3% of the total number of elements. We remark that the halfedge data structure has to be recomputed after mesh simplification. Table 6 presents the results obtained with the algorithm for the simplification of elements with valence pattern $3-3-3-3$. Run times

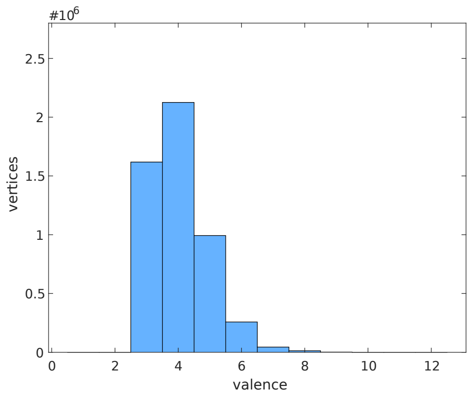

(a) Valence distribution before simplification

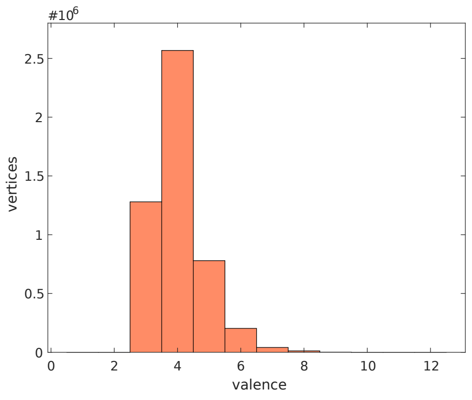

(b) Valence distribution after simplification

Figure 12: Distribution of the vertex valences in the DMC mesh before simplification in blue and after in red.

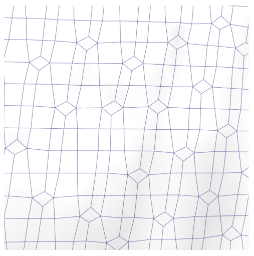

(a) DMC mesh

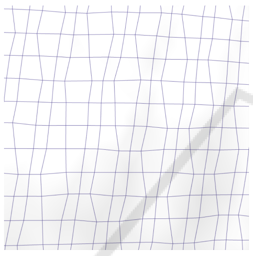

(b) DMC after simplification

Figure 13: DMC mesh after removing elements with valence pattern $3-X-3-Y$ and $3-3-3-3$

are comparable to the previous case, also eliminating a similar number of elements, except for the case of the human torso with iso-value 700, named body in the table. Due to the geometric properties of the iso-surface, the body surface does not have many elements with this valence pattern.

6 CONCLUSIONS

We presented a parallel implementation of the DMC algorithm which efficiently processes volume data consisting of hundreds of millions of voxels. The DMC meshes are topologically consistent across cell borders. This is due to the fact that we compute the intersection of the iso-surface with the cells using the asymptotic decider to solve ambiguities. The output of the algorithm is a quadrilateral mesh stored in a halfedge data structure. We use the fact that the data is already on the GPU device and perform some mesh simplification by eliminating vertices and quadrilaterals with valence pattern $3-X-3-Y$, $X,Y \geq 5$ and $3-3-3-3$. This way vertices in the DMC mesh have better valence distribution. In the implementation geometric constraints for the simplification were not considered. The DMC algorithm generate meshes with a better element quality than the standard MC.

REFERENCES

Attali, D., Cohen-Steiner, D., and Edelsbrunner, H. (2005). Extraction and simplification of iso-surfaces in tandem. In *Proceedings of the Third Eurographics Symposium on Geometry Processing*, SGP '05, Aire-la-Ville, Switzerland, Switzerland. Eurographics Association.

Chen, J., Jin, X., and Deng, Z. (2015). Gpu-based polygonization and optimization for implicit surfaces. *Vis. Comput.*, 31(2):119–130.

Chernyaev, E. V. (1995). Marching cubes 33: Construction of topologically correct isosurfaces. Technical report.

Cignoni, P., Ganovelli, F., Montani, C., and Scopigno, R. (2000). Reconstruction of topologically correct and adaptive trilinear isosurfaces. *Computers & Graphics*, 24:399–418.

Custodio, L., Etiene, T., Pesco, S., and Silva, C. (2013). Practical considerations on marching cubes 33 topological correctness. *Computers & Graphics*, 37(7):840 – 850.

D'Agostino, D. and Seinstra, F. J. (2015). A parallel isosurface extraction component for visualization pipelines executing on gpu clusters. *J. Comput. Appl. Math.*, 273(C):383–393.

de Bruin, P. W., Vos, F. M., Post, F. H., Frisken-Gibson, S. F., and Vossepoel, A. M. (2000). Improving triangle mesh quality with surfacenets. In *Medical Image Computing and Computer-Assisted Intervention – MICCAI 2000*, pages 804–813, Berlin, Heidelberg. Springer Berlin Heidelberg.

Dupuy, G., Jobard, B., Guillon, S., Keskes, N., and Komatitsch, D. (2010). Parallel extraction and simplification of large isosurfaces using an extended tandem algorithm. *Comput. Aided Des.*, 42(2):129–138.

Dürst, M. J. (1988). Re: Additional reference to ”marching cubes”. *SIGGRAPH Comput. Graph.*, 22(5):243–.

Etiene, T., Nonato, L. G., Scheidegger, C., Tienry, J., Peters, T. J., Pascucci, V., Kirby, R. M., and Silva, C. T. (2012). Topology verification for isosurface extraction. *IEEE Transactions on Visualization and Computer Graphics*, 18(6):952–965.

Freitag, L. A. and Knupp, P. M. (2002). Tetrahedral mesh improvement via optimization of the element condition number.

Gibson, S. F. F. (1998). Constrained elastic surface nets: Generating smooth surfaces from binary segmented data. In *Medical Image Computing and Computer-Assisted Intervention — MICCAI'98*, pages 888–898, Berlin, Heidelberg. Springer Berlin Heidelberg.

Grosso, R. (2016a). Construction of topologically correct and manifold isosurfaces. *Computer Graphics Forum*, 35(5):187–196.

Grosso, R. (2016b). tmc. `https://github.com/rogrosso/tmc`.

Grosso, R. (2017). An asymptotic decider for robust and topologically correct triangulation of isosurfaces. In *Proceedings of the Computer Graphics International Conference*, CGI '17, pages 39:1–39:5, New York, NY, USA. ACM.

Ju, T., Losasso, F., Schaefer, S., and Warren, J. (2002). Dual contouring of hermite data. In *Proceedings of the 29th Annual Conference on Computer Graphics and Interactive Techniques (SIGGRAPH 2002)*, pages 339–346. ACM Press.

Kazhdan, M., Klein, A., Dalal, K., and Hoppe, H. (2007). Unconstrained isosurface extraction on arbitrary octrees. In *Proceedings of the Fifth Eurographics Symposium on Geometry Processing*, pages 125–133.

Lewiner, T., Lopes, H., Vieira, A. W., and Tavares, G. (2003). Efficient implementation of marching cubes' cases with topological guarantees. *Journal of Graphics Tools*, 8(2):1–15.

Löffler, F. and Schumann, H. (2012). Generating smooth high-quality isosurfaces for interactive modeling and visualization of complex terrains. In *VMV*.

Lopes, A. and Brodlie, K. (2003). Improving the robustness and accuracy of the marching cubes algorithm for isosurfacing. *IEEE Transactions on Visualization and Computer Graphics*, 9:2003.

Lorensen, W. E. and Cline, H. E. (1987). Marching cubes: A high resolution 3d surface construction algorithm. *SIGGRAPH Comput. Graph.*, 21(4):163–169.

M. Knupp, P. (2000). Achieving finite element mesh quality via optimization of the jacobian matrix norm and associated quantities. part i—a framework for surface mesh optimization. *Int. J. Numer. Meth. Engng*, 48:401–420.

Matveyev, S. V. (1999). Marching cubes: surface complexity measure. In *Proceedings of SPIE - The International Society for Optical Engineering*, volume 3643, pages 220–225.

Montani, C., Scateni, R., and Scopigno, R. (1994). A modified look-up table for implicit disambiguation of marching cubes. *The Visual Computer*, 10(6):353–355.

Natarajan, B. K. (1994). On generating topologically consistent isosurfaces from uniform samples. *The Visual Computer*, 11(1):52–62.

Nielson, G. M. (2003). On marching cubes. *IEEE Transactions on Visualization and Computer Graphics*, 9(3):283–297.

Nielson, G. M. (2004). Dual marching cubes. In *Proceedings of the Conference on Visualization '04*, VIS '04, pages 489–496, Washington, DC, USA. IEEE Computer Society.

Nielson, G. M. and Hamann, B. (1991). The asymptotic decider: Resolving the ambiguity in marching cubes. In *Proceedings of the 2Nd Conference on Visualization '91*, VIS '91, pages 83–91, Los Alamitos, CA, USA. IEEE Computer Society Press.

Pasko, A., Pilyugin, V., and Pokrovskiy, V. (1988). Geometric modeling in the analysis of trivariate functions. *Computers & Graphics*, 12(3):457 – 465.

Rashid, T., Sultana, S., and Audette, M. A. (2016). Watertight and 2-manifold surface meshes using dual contouring with tetrahedral decomposition of grid cubes. *Procedia Engineering*, 163:136 – 148. 25th International Meshing Roundtable.

Renbo, X., Weijun, L., and Yuechao, W. (2005). A robust and topological correct marching cube algorithm without look-up table. In *Proceedings of the The Fifth International Conference on Computer and Information Technology*, CIT '05, pages 565–569, Washington, DC, USA. IEEE Computer Society.

Schaefer, S., Ju, T., and Warren, J. (2007). Manifold dual contouring. *IEEE Transactions on Visualization and Computer Graphics*, 13(3).

Schaefer, S. and Warren, J. (2004). Dual marching cubes: Primal contouring of dual grids. In *Computer Graphics and Applications, 2004. PG 2004. 12th Pacific Conference on*, pages 70–76. IEEE Computer Society.

Ulrich, C., Grund, N., Derzapf, E., Lobachev, O., and Guthe, M. (2014). Parallel iso-surface extraction and simplification. In *WSCG 2014 : Communication Papers Proceedings*, pages 361–368. Vaclav Skala – Union Agency, Plzen.

Zhang, N., Hong, W., and Kaufman, A. (2004). Dual contouring with topology-preserving simplification using enhanced cell representation. In *Proceedings of the Conference on Visualization '04*, pages 505–512.